www.amlett.com, www.vbripress.com/aml, DOI: 10.5185/amlett.2015.5831 Published online by the VBRI Press in 2015

Silver ion conducting characteristics of a polyethylene oxide-based composite polymer electrolyte and application in solid state batteries

S. Amudha*, S. Austin Suthanthiraraj

Department of Energy, University of Madras, Guindy Campus, Chennai 600025, India

*Corresponding author. Tel: (+91) 9994689145; E-mail: amudha.sbs@gmail.com

Received: 02 February 2015, Revised: 08 May 2015 and Accepted: 15 June 2015

ABSTRACT

The matrix embracing a combination of polyethylene oxide [PEO] as the host polymer component and silver trifluoromethane sulfonate [$AgCF_3SO_3$] (also known as silver triflate) as the dopant salt yielding a composite polymer electrolyte [CPE] with varying compositions based on rich contents of Oxygen/Metal [O/M] ratio has been prepared in the form of thin film specimens using solution casting technique and examined for its application in a solid state battery configuration as a test cell. Such composite polymeric films optimized using electrical conductivity studies have provided realization of a maximum electrical conductivity value of 2.9×10^{-5} Scm^{-1} at room temperature (298 K) whereas their temperature-dependent electrical conductivity is found to obey the Arrhenius behavior. Silver ionic transference number (t_{Ag}^{+}) data for these polymeric composites were indomitable using ac/dc polarization technique whereas the occurrence of a transition of phase in accordance with structural and thermal parameters could be investigated by means of X-ray diffraction (XRD) and differential scanning calorimetric (DSC) analyses. The morphological and compositional analyses were carried out by employing scanning electron microscopy (SEM), field emission scanning electron microscopy (FESEM) and energy dispersive X-ray spectroscopy (EDX) as analytical tools. Electrochemical cells have been fabricated with the common cell configuration Ag|CPE|(I_2+G+CPE) and relevant cell parameters evaluated in terms of their discharge characteristics under a constant load of 1 MΩ at room temperature.

Keywords: Electrical conductivity; polymeric film; X-ray diffraction; device parameters.

Introduction

Composite polymer electrolytes (CPEs) based on polyethylene oxide (PEO) have become incredibly important owing to their certain promising features for many devices such as high energy density batteries, solid state sensors, fuel cells, cell phones, smart credit cards, supercapacitors and electrochromic windows (ECWs) etc. in recent years **[1]**. The most significant advantage of composite polymer electrolytes (CPEs) involves their feasibility of purge of leakage and in general CPEs are known to exhibit proficient electrochemical characteristics such as desirable ionic conductivity, interfacial stability, transport and mechanical properties **[2]**. Usually, CPEs may be made in the form of thin films on account of their appreciably high room temperature electrical conductivity and good mechanical stability aspects which could be appropriately controlled by varying either the polymer or salt concentration in the case of polymer-salt matrices **[3]**. Myriad composite polymer electrolyte exhibit this kind of behavior and some of them include polyvinylidene fluoride-hexafluoro propylene (PVdF-HFP) **[4]**, polyethylene oxide (PEO) **[5]**, polyethylene glycol (PEG) **[6]**, polyvinyl chloride (PVC) **[7]**, polypropylene glycol (PPG) **[8]**, polyethylene malonate (PEM) **[9]** and polyvinylpyrrolidone (PVP) **[10]** respectively.

Among them polyethylene oxide (PEO) is one of the most significant polymer which exhibits electrical conductivity values in the range 10^{-10} to 10^{-9} Scm^{-1} at ambient temperatures and hence in order to enhance ion-conducting properties of a polymeric system numerous modifications involving incorporation of suitable salts based on lithium, imidazolium, zinc, sodium and potassium etc **[11-15]** were introduced. At first Armand *et al.* proposed the structural, morphological and transport properties of polyethylene oxide with alkali metal salts **[16]**. Furthermore, several reports regarding ion conducting behavior of PEO-based polymer electrolytes and extensively their application in batteries are available in literature **[17, 18]**.

In view of these facts the current research work has been implemented in order to comprehend the effective interaction of polyethylene oxide (PEO)-rich polymeric

composition in conjunction with silver triflate ($AgCF_3SO_3$) salt by dissolving them using dimethyl formamide (DMF) as the common solvent. PEO is a typical polymer host having a helical structure with C-O bonds in trans- mode and C-C bonds in gauche configuration while in this geometry cations may be located in every twirl of the helix which is synchronized by three ether oxygen. Generally, PEO polymer contains both amorphous and crystalline phases with highly ordered chain structure but the dominant presence of crystalline phase impedes the movement of ions through segmental motion thereby resulting in a higher degree of crystallinity [**19-22**].

Therefore, with a view to decrease the degree of crystallinity, the dopant salt namely $AgCF_3SO_3$ has been introduced into the PEO polymer matrix which may effectively enable the host polymer to exhibit the inherent property of an enhanced ionic conductivity. Silver triflate is chosen as a dopant salt owing to its non-hazardous, thermally firm, exceedingly resistive to oxidation process and non-susceptible to ambient humidity nature. The use of $AgCF_3SO_3$ salt with appreciably high lattice energy is expected to prevent the reduction of silver ions and reveal better performance in terms of electrochemical stability and high ionic conductivity **[23]**. Interestingly, Ag^+ cations in $AgCF_3SO_3$ would coordinate with the ether oxygen of PEO which may dissolve major concentration of ions in the chosen silver salt and facilitate ion dissociation process to occur **[24]**. This in turn would increase the movement of ions and decrease the degree of crystallinity in pure PEO polymer whereas reduction in degree of crystallinity favors inter-chain and intra-chain hoping of ions thereby enabling conducting pathways which enhances ionic conduction **[25]**.

The main aim of this research work is therefore to understand the effect of silver triflate on ion conducting characteristics of the PEO based composite polymer electrolyte using a diverse solvent namely dimethyl formamide (DMF). Upto now, most of the researchers employed acetonitrile (ACN or CH_3CN) as the frequent solvent to dissolve PEO and $AgCF_3SO_3$, however in this work a new approach has been undertaken i.e., by considering dimethyl formamide (DMF or $(CH_3)_2NC(O)H$) as the common solvent. In general, DMF is an aprotic and hydrophilic solvent exhibiting characteristic molar mass, wavelength, density and boiling point of 73.09 g mol^{-1}, 270 nm, 948 mg mL^{-1} and 425-427 K respectively in comparison with acetonitrile whereas the chemical response between PEO and $AgCF_3SO_3$ is also expected to increase by using DMF as the solvent. Accordingly, during the present study, DMF has been chosen as the solvent for the preparation of composite polymer electrolyte films by means of solution casting technique as this endeavor aims at understanding the relevant electrochemical properties by employing certain analytical tools. such as electrical conductivity measurements, X-ray diffraction (XRD) analysis, differential scanning calorimetric (DSC) studies, scanning electron microscopic (SEM) analysis, field emission scanning electron microscopy (FESEM) and energy dispersive X-ray spectroscopic (EDX) techniques.

Experimental

Materials and methods

Commercially available polyethylene oxide (PEO) $[(C_2H_4O)_n.H_2O]$ with a high molecular weight of $M_w \approx 5000000$ and silver trifluoromethane sulfonate ($AgCF_3SO_3$) (silver triflate or AgTr) of $M_w \approx 256.94$ were procured from Sigma Aldrich. Essentially, DMF (also known as dimethylmethanamide), a hydrophilic and aprotic solvent with high boiling point around 425-427 K was purchased from Merck and used as the common solvent. The specimens of silver ion conducting composite polymer electrolyte films were prepared by coalescing PEO as the host polymer and $AgCF_3SO_3$ as the dopant salt by the well-known experimental process namely solution casting technique. Preceedingly, silver triflate was dried under vacuum line at 393 K for 1 h. Subsequently, appropriate amounts of polymer and salt were taken in varying values of O/M ratio i.e. Oxygen-to-Metal ratio because oxygen atom in PEO polymer interacts well with Ag^+ metal ion in $AgCF_3SO_3$ salt. Various compositions of $(PEO)_x$:$AgCF_3SO_3$ (where x = 50, 60, 70, 80, 90 and 100 respectively) were taken in a 100 ml beaker and the mixture was dissolved in DMF followed by constant stirring at 323 K for 4 h in order to obtain a homogeneous solution. The solution thus acquired was poured into glass petridishes and dried in a vacuum oven at 333 K for 24 h to confiscate the traces of solvent and dampness. Free standing, stable thin film composite polymer electrolyte specimens were obtained upto 50:1 (O/M ratio) below which the film formation is found to be very much intricate. The average thickness of these films computed by air wedge technique was determined to lie in the range 50-60 µm and all the specimens were stored in a vacuum desiccator for further characterization studies.

Characterization

The complex impedance data were collected and analyzed systematically using a computer-interfaced Hewlett-Packard Model HP4284A Precision LCR Meter in a linear frequency (f) range of 20 Hz^{-1} MHz with an applied amplitude of 500 mV for freshly prepared specimens of PEO-$AgCF_3SO_3$ CPE at room temperature (298 K) over the region 298 – 323 K approximately at 5 K hiatus for the typical $(PEO)_{60}$:$AgCF_3SO_3$ composite polymer electrolyte film itself. The temperature of the specimen was measured with the aid of a thermocouple kept in thermal contact with the specimen under test. The CPE films were sandwiched between a pair of silver electrodes of 8 mm diameter each in pellet form made from pure silver powder at a pelletizing pressure of about 200 MPa. Prior to each measurement the specimen could be calibrated for open circuit and short circuit corrections in order to eliminate the effect of stray capacitance of the cell probes. The experiment was repeated four times and the error involved was estimated to be approximately ± 6.7 %. After computing complex impedance studies the cell was polarized by a dc potential with an applied cell voltage of 50 mV and the resulting current was monitored as a function of time with the aid of a Keithley Model 2400 Sourcemeter at room temperature until a steady-state was reached. An impedance analysis was carried out immediately after the application of the dc

voltage in order to evaluate the effect of changes taking place across the sample/electrode interface.

Structural studies were performed at room temperature (293 K) using a Bruker D8 Advance X-ray Diffractometer with monochromatic CuKα (λ=1.5406 Å) radiation source operated at the voltage of 40 kV and current of 30 mA over the scattering angle ranging from 2θ = 10-80º with a step size of 0.02º/min.

Thermal characteristics of composite polymer electrolyte samples of various compositions have been investigated with the aid of a DSC 200 F3 Maia model thermal analyzer (NETZSCH-make) under nitrogen atmosphere at a heating rate of 10 degree/min and melting temperatures and enthalpies were determined from positions of observed DSC peaks and their appropriate areas, respectively. For each DSC measurement, CPE films having an approximate weight of 5 to 10 mg were sealed in aluminum pans and an empty aluminum pan was used as the reference. Both the pans were placed in a heater and the whole system monitored by a computer. As and when the temperature increases the computer has been programmed for the drawing of the relevant DSC curve by plotting temperature along X-axis and heat flow along Y-axis. Here nitrogen (N_2) gas has been used in order to avoid moisture content within the sample.

The surface morphology of the composite polymer electrolyte film was observed using a SEM, Hitachi-S 3400 Model (Japan) with an accelerating voltage of 10 kV and the depiction was obtained by fracturing the sample in liquid nitrogen. It was then vacuum-dried, sputter coated with gold particles upto 30 seconds to minimize electrostatic charging and attached to a sample holder with the aid of conductive copper tapes.

The field emission scanning electron microscopic (FESEM) analysis was carried out using a SU6600 Model scanning electron microscope with an accelerating voltage of 5,000 V and emission current of 28000 nA. The CPE films were coated with gold so as to make them electrically conducting and mounted on circular aluminum stubs with the help of double side sticky cello tapes. Energy dispersive X-ray spectroscopy (EDX) picture was traced out using the EDAX analyzer attached to the FESEM instrument itself.

Fabrication of solid state battery cell

Solid state electrochemical cells were fabricated with the general configuration anode/polymer electrolyte/cathode. Generally, anode in the case of a silver battery must be able to provide silver ions and pure silver powder has therefore been made in the form of a pellet using a pelletizer and employed as the anode component. For the preparation of the cathode material, iodine (I_2), graphite (G) and composite polymer electrolyte film (CPE) were taken in the weight ratio of 3:3:1 in a mortar and ground together along with a small amount of acetone and made in the form of a thin pellet at a pelletizing pressure of about 250 MPa. The best conducting composite polymer electrolyte film was sandwiched between the cathode material and Ag pellet. The open-circuit voltage (OCV), short-circuit current (SCC) and cell potential measurements were carried out with the help of a high impedance MS8265 Model Digital Multimeter whereas discharge characteristics of the cell were monitored without load and under a constant load of 1 MΩ connected in parallel and in series to the load to measure OCV and SCC respectively as a function of time.

Results and discussion

Electrical conductivity results

The behavior of electrical conductivity of all the five different CPE films was scrutinized by means of electrochemical impedance spectroscopy (EIS) and **Fig. 1** shows the experimental and fitted Nyquist plot curves obtained at room temperature for $(PEO)_x$:$AgCF_3SO_3$ (where x = 50, 60, 70, 80 and 90 respectively) complexes. A careful examination of these Nyquist plots shows two diverse regions i.e. a depressed semicircle is observed at higher frequencies ensued by a tilted spike at lower frequencies. The higher frequency depressed semicircle corresponds to the conduction mechanism of ions whereas low frequency spike represents electrode (Ag^+) electrolyte (CPE film) polarization effects. In addition, the tilted spike may also tend to appear due to the accumulation of free charges at the electrical double layer capacitance (EDLC) formed between Ag^+ and CPE film in a planar geometry[26]. The bulk resistance R_b of the complexed PEO polymer electrolyte film has been determined from the fitted results using Z-Sim Demo Software with respect to the intercepts of high frequency semicircular arc at Z' axis (real axis) and the value of electrical conductivity (σ) was calculated using the equation,

$$\sigma \cdot \approx \frac{t}{A \times R_b} \qquad (1)$$

where, R_b is the bulk resistance, t and A are the thickness and area of composite polymer electrolyte film respectively. The electrical conductivity of pure PEO polymer electrolyte film at room temperature (298 K) is found to be 3.25×10^{-10} Scm^{-1}as reported earlier **[27]**.

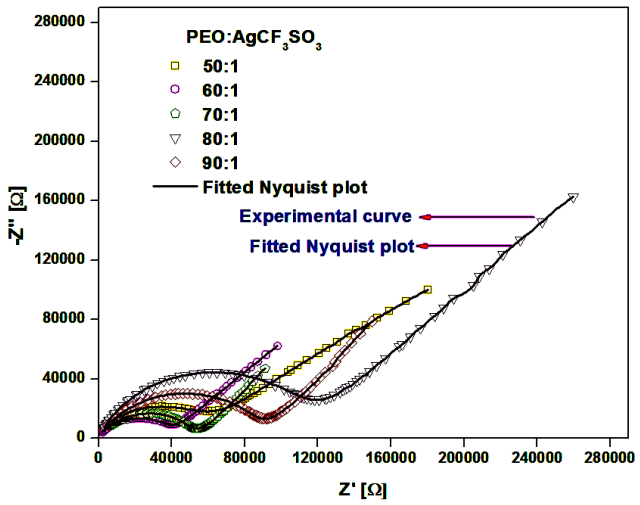

Fig. 1. Experimental and fitted Nyquist plots obtained at room temperature for the $(PEO)_x$: $AgCF_3SO_3$ (where x = 50, 60, 70, 80 and 90 respectively) complexes.

Accordingly, the values of room temperature electrical conductivity estimated for $(PEO)_{50}$:$AgCF_3SO_3$, $(PEO)_{60}$:$AgCF_3SO_3$,$(PEO)_{70}$:$AgCF_3SO_3$,$(PEO)_{80}$:$AgCF_3S_3$

and $(PEO)_{90}$:$AgCF_3SO_3$ complexes are found to be 1.2×10^{-5}, 2.9×10^{-5}, 2.4×10^{-5}, 6.2×10^{-6} and 7.7×10^{-6} Scm^{-1} respectively. In comparison with pure PEO polymer electrolyte film the salt added $(PEO)_{60}$:$AgCF_3SO_3$ composite polymer electrolyte film shows an increase in magnitude by five orders and such steep increase in conductivity may be attributed to the feasibility of reduction in the crystallinity (χ_c) of the PEO polymer host and also the coordinative interaction taking place between ether oxygen of PEO and Ag^+ cation released from $AgCF_3SO_3$. The variation of room temperature electrical conductivity and degree of crystallinity (χ_c) as calculated from XRD data for the series of composite polymer electrolyte films as a function of polymer concentration is graphically depicted in **Fig. 2**.

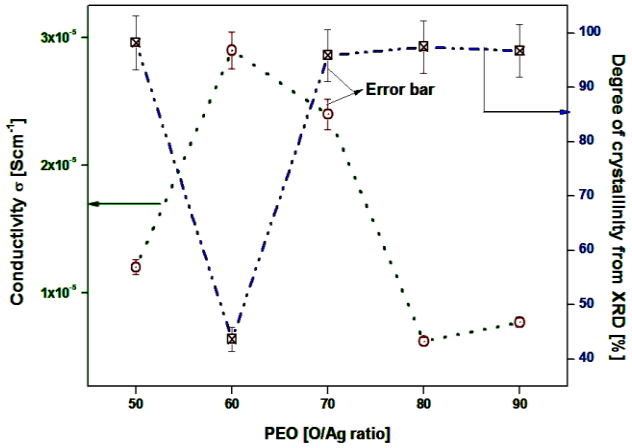

Fig. 2. Room temperature electrical conductivity and degree of crystallinity of PEO:$AgCF_3SO_3$ composite polymer electrolyte films as a function of polymer concentration at room temperature [298 K].

The observed characteristic electrochemical impedance response for the $(PEO)_{60}$:$AgCF_3SO_3$ composite polymer electrolyte film at five different temperatures i.e. 303, 308, 313, 318 and 323 K is presented in **Fig. 3**.

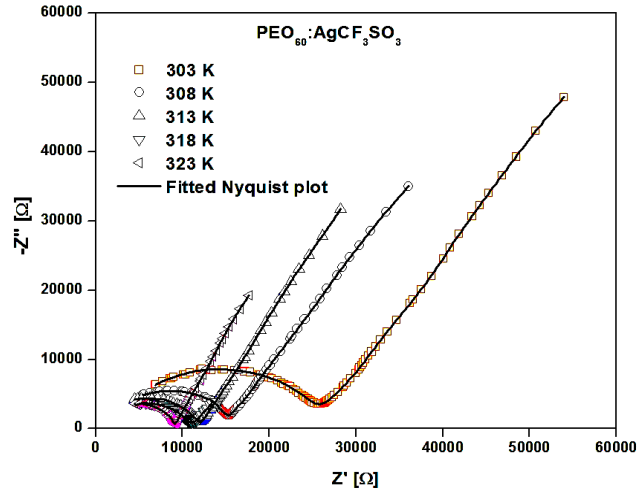

Fig. 3. Experimental and fitted Nyquist plots obtained at five different temperatures for $(PEO)_{60}$: $AgCF_3SO_3$ composite polymer electrolyte film.

The curves obtained were fitted as enlightened above and the corresponding conductivity values are found to be 3.8×10^{-5}, 5.8×10^{-5}, 7.1×10^{-5}, 9.4×10^{-5} and 1.1×10^{-4} Scm^{-1}, respectively. It is quite evident from the above figure that as temperature increases, bulk resistance (R_b) decreases and conductivity begins to increase and this kind of behavior may be attributed as due to the occurrence of an abrupt increase in the vibrational motion taking place within the backbone and alongside chains of the PEO polymer matrix too. This sort of an increased vibration brings those Ag^+ ions in the coordination sites to hop from one site to another and as a result the fraction of free volume of CPE film tends to increase. This aspect may also give rise to translational motion of ions and hence the increase in temperature is expected to be associated with an increase in the free volume as well as relevant ionic and segmental mobility features of the chosen polymer electrolyte as well.

Fig. 4 shows the plots of dielectric constant (ε') as a function of logarithm of frequency at different temperatures for the typical $(PEO)_{60}$:$AgCF_3SO_3$ composite polymer electrolyte film. The dielectric constant may be calculated using the equation,

$$\varepsilon' \approx Cd/\varepsilon_0 A \qquad (2)$$

where, d, ε_0 and A denote the thickness, dielectric permittivity or permittivity of free space and area of cross-section of the sample and hence C may be evaluated using the equation,

$$C \approx \frac{Z\cos\theta}{Z^2\times 2\pi f} \qquad (3)$$

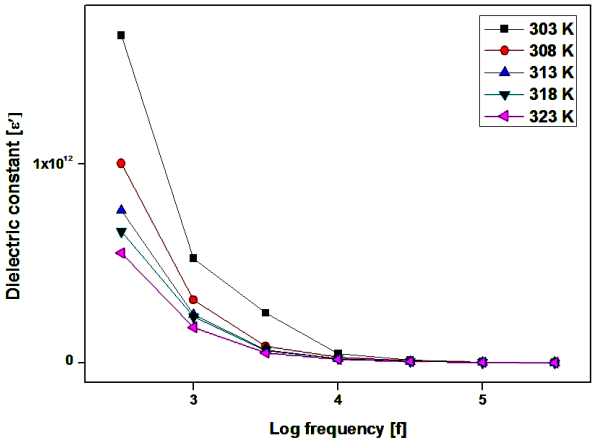

Fig. 4. Dielectric constant as a function of logarithm of frequency at five different temperatures for $(PEO)_{60}$:$AgCF_3SO_3$ composite polymer electrolyte film.

From **Fig. 4** it is quite evident that the value of dielectric constant becomes large at low frequencies and vice-versa at higher frequencies and tends to get overlapped at low frequencies at various temperatures. This feature may be due to the space charge effect and ionic polarization occurring at lower frequencies whereas at higher frequencies the relevant polarization effect decreases progressively **[28]**.

The variation of the observed electrical conductivity (σ) with respect to inverse of absolute temperature (1/T)

involving the temperature range 298-323 K for the typical $(PEO)_{60}$:$AgCF_3SO_3$ composite polymer electrolyte film is shown in **Fig. 5**. The graph exhibits Arrhenius behavior and dependence of conductivity with respect to temperature follows the relationship,

$$\sigma \approx \sigma_0 \exp\left(\frac{-E_a}{kT}\right) \quad (4)$$

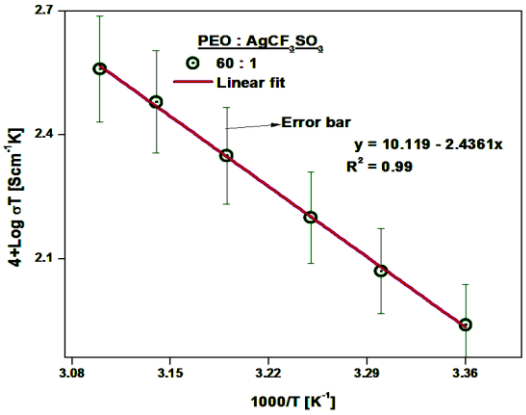

Fig. 5. Variation of electrical conductivity as a function of inverse of absolute temperature for $(PEO)_{60}$:$AgCF_3SO_3$ composite polymer electrolyte film.

where, σ_0 is the pre-exponential factor, E_a the activation energy and k is the Boltzmann constant. The observed plot is fitted in a linear form (y = A+Bx) and from the estimated slope of this plot, the value of activation energy E_a could be calculated as portrayed in **Table 1**.

Table 1. Activation energy and adjacent R^2 values obtained for the $(PEO)_{60}$:$AgCF_3SO_3$ composite polymer electrolyte film.

Frequency	Adjacent R-square value obtained from frequency dependent Arrhenius plot	Frequency-dependent activation energy, E_a (eV)	Activation energy from complex impedance analysis, E_a (eV)	Adjacent R-square value derived from complex impedance analysis
10 kHz	0.92	0.42		
1 kHz	0.91	0.47	0.48	0.99
500 Hz	0.93	0.52		
50 Hz	0.96	0.47		

The temperature dependence of electrical conductivity observed for the $(PEO)_{60}$:$AgCF_3SO_3$ composite polymer electrolyte film specimen over the temperature window 298-323 K at four different frequencies namely 10 MHz, 1 MHz, 500 Hz and 50 Hz respectively is depicted in **Fig. 6**.

These graphs have also been fitted linearly as mentioned above and the set of calculated activation energy values are presented in **Table 1**. From **Table 1** it is evident that the present activation energy value is found lies in the range 0.42-0.52 eV and that such low activation energy values may be due to the possible decrease in the crystalline nature of the chosen polymer-salt complexes. The fact that both the activation energy values evaluated from complex impedance analysis and frequency-dependent electrical conductivity data are quite comparable with one another and implies that $AgCF_3SO_3$ salt liberates more number of Ag^+ cations in order to interact with ether oxygen of PEO which in turn may provide conducting pathways and hence the observed conductivity increases.

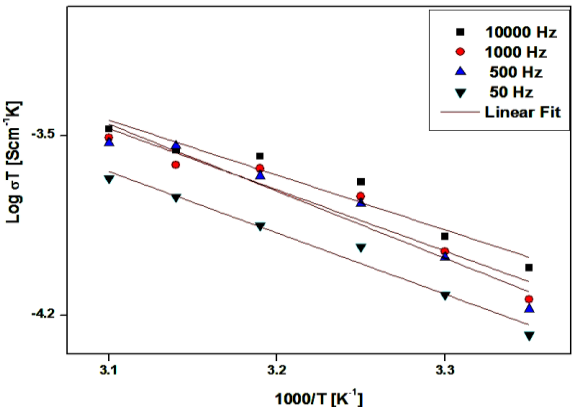

Fig. 6. Variation of electrical conductivity as a function of inverse of temperature at 10 MHz, 1 MHz, 500 Hz and 50 Hz for (PEO)60:Ag CF3 SO3 composite polymer electrolyte film.

The silver ionic transference number (t_{Ag^+}) corresponding to cationic mobilities in the case of $(PEO)_{60}$: $AgCF_3SO_3$ composite polymer electrolyte film sample was measured using ac/dc polarization method and calculated using the relationship

$$t_{Ag^+} \approx \frac{I_s(\Delta V - I_0 R_0)}{I_0(\Delta V - I_s R_s)} \quad (5)$$

where, ΔV represents the constant dc polarization potential applied across the cell (~ 50 mV), I_0 and I_s represent the initial and steady-state current noted from dc polarization whereas R_0 and R_s denote the initial and steady-state interfacial resistance values extorted from Nyquist plots before and after dc polarization as depicted in **Fig. 7(a)**. The values of (t_{Ag^+}) thus obtained have been used to plot the relevant graphs of normalized polarization current with respect to time for the $(PEO)_{60}$:$AgCF_3SO_3$ composite polymer electrolyte film specimen during direct current polarization of the cell assembled with Ag/CPE/Ag as shown in **Fig. 7(b)** and the value of t_{Ag^+} at room temperature was subsequently found to be 0.78. This value may be attributed as due to the feasibility of dissociation of Ag^+ cations from the coordinating ether oxygen of PEO polymer and charge transport within the composite film is therefore ascribable mainly due to cationic motion only **[29]**.

X-ray diffraction (XRD) data

Fig. 8(a) shows the room temperature X-ray diffraction (XRD) patterns of $(PEO)_x$:$AgCF_3SO_3$ (where, x = 90, 80, 70, 60 and 50 respectively) and pure PEO and pure silver triflate samples. Pure PEO shows characteristic diffraction peaks at 2θ = 19.16° and 23.3° which may correspond to [120] and [112] reflection planes of a monoclinic crystal system. These main peaks may be due to the presence of multiphase structure consisting of both crystalline and amorphous phases as well as ordering of polyether side chains within the host PEO polymer electrolyte. These X-ray diffractograms also exhibit a halo peak centered at 18.7° and two shoulder peaks at 26.3° and 26.9° respectively. Furthermore, it is understood that after the incorporation of $AgCF_3SO_3$ salt the intensity of prominent

diffraction peaks gets reduced in comparison with pure PEO and also the position of peaks begins to shift slightly as shown in **Fig. 8(b).**

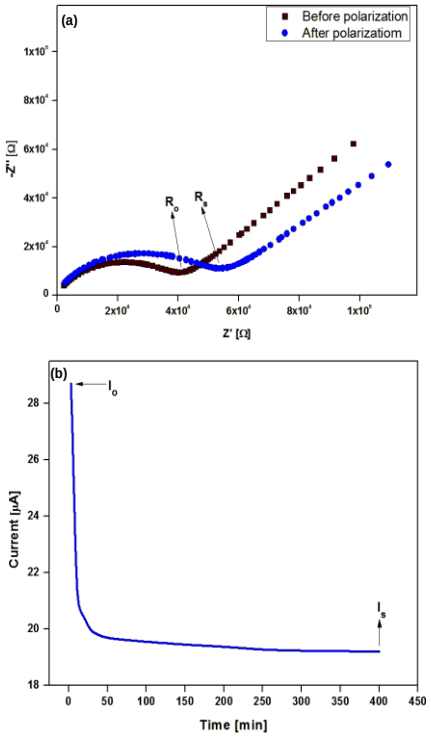

Fig. 7. (a) Complex impedance plots obtained for $(PEO)_{60}$: $AgCF_3SO_3$ composite polymer electrolyte film before and after polarization and **(b)**. Variation of current with respect to time for the cell assembled with Ag/(PEO)60: AgCF3SO3/Ag at an applied potential (ΔV) of 50 mV at 298 K.

This sort of shift appearing in the position of peaks may be due to the possible transformation from crystalline to amorphous phase and in view of the fact that no diffraction peak corresponding to pure $AgCF_3SO_3$ is found to appear in the XRD pattern for the complex. This indicates the feasibility of complete dissolution of PEO polymer and $AgCF_3SO_3$ salt and absence of any excessive uncomplexed salt within the composite polymer electrolyte (CPE) sample.

In this particular CPE film specimen, the Ag^+ cation may tend to disturb the ordering of PEO side chains thereby resulting in an increased amorphous nature and the results inferred from the appropriate X-ray pattern is in good agreement with the present conductivity measurements wherein the observed conductivity behavior is correlated to the amorphous phase of the CPE sample. The crystallite size, L of the series of specimens of $(PEO)_x$:$AgCF_3SO_3$ complex ($50 \leq x \leq 90$) has been calculated from the full-width half maximum (FWHM) of X-ray pattern perpendicular to [120] plane using Debye-Scherrer formula.

$$L \approx \frac{k\lambda}{\beta Cos\theta} \qquad (6)$$

where, k is the Scherrer shape factor (k = 0.94), λ the wavelength of X-ray radiation used which is 1.5406 Å, β the full width at half maximum intensity of the prominent diffraction peak, θ is the Bragg diffraction angle. The particle size data obtained for the various samples of $(PEO)_x$: $AgCF_3SO_3$ complex are found to be in the range 44.4 - 27.2 nm and the average inter-chain separation (R) of the CPE film has been estimated using the equation,

$$R \approx \frac{5\lambda}{8Sin\theta} \qquad (7)$$

The degree of crystallinity(χc) of the polymer electrolyte sample has been calculated on the basis of Hermans-Weidinger method as reported earlier **[31]**.

$$\chi_c \approx \frac{A_{crystalline}}{A_{crystalline} + kA_{amorphous}} \qquad (8)$$

where, $A_{crystalline}$ and $A_{amorphous}$ are the total areas under crystalline peaks noticed at 19.16°, 23.3°, 26.3° and 26.9° and area under amorphous halo at 18.7° respectively and k is a constant equal to unity.

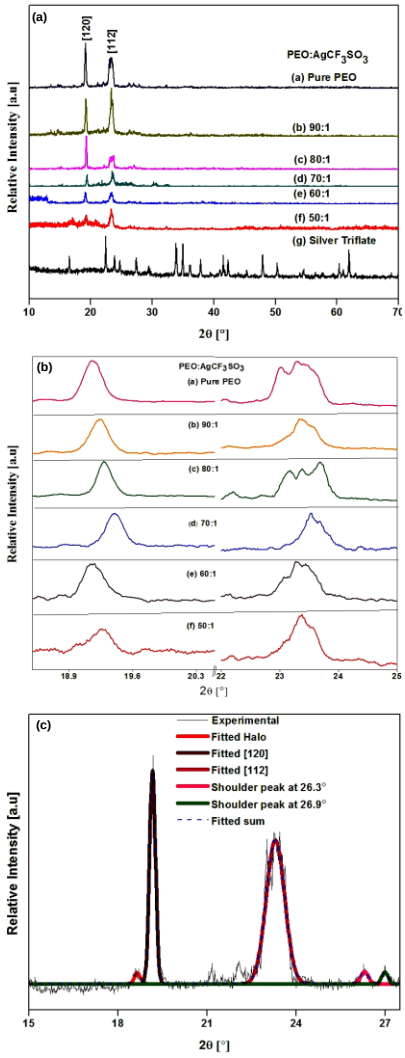

Fig. 8. (a) X-ray diffraction patterns obtained for different compositions of $(PEO)_x$: $AgCF_3SO_3$ complexes, (b) Shifts taking place in the position of prominent X-ray diffraction peaks on variation in PEO concentration for $(PEO)_x$: $AgCF_3SO_3$ complexes and (c) Deconvoluted X-ray diffraction patterns of pure PEO showing Gaussian fittings of halo, [120], [112] and the shoulder peaks at 26.3 and 26.9°.

The areas under crystalline and amorphous peaks were calculated by deconvoluting the X-ray diffraction pattern using Origin Pro 8 peak separation software and the deconvoluted XRD pattern of pure PEO polymer is shown in **Fig. 8(c)**.

The calculated value of degree of crystallinity (χ_c) is found to decrease from 98.3 % for pure PEO polymer to as low as 43.6 % for $(PEO)_{60}$:$AgCF_3SO_3$ composite polymer electrolyte film. Diverse structural parameters such as d-spacing profile, full width half maximum (FWHM), crystallite size (L), inter-chain separation (R) and degree of crystallinity (χ_c) obtained for pure PEO and PEO_x:$AgCF_3SO_3$ polymer electrolyte films are presented in **Table 2**.

Table 2. Structural parameters obtained for pure PEO and $(PEO)_x$:$AgCF_3SO_3$ composite polymer electrolyte films.

Films	Peak position 2θ [°]	Interplanar spacing d [Å]	Full width half maximum β [radians]	Crystallite size L [nm]	Interchain separation R [Å]	Degree of crystallinity from XRD χ_c [%]
Pure PEO	19.16	4.63	3.49×10^{-3}	42.1	5.79	98.3
PEO_{90}: $AgCF_3SO_3$	19.23	4.62	4.54×10^{-3}	32.4	5.77	96.7
PEO_{80}: $AgCF_3SO_3$	19.29	4.6	3.31×10^{-3}	44.4	5.75	97.4
PEO_{70}: $AgCF_3SO_3$	19.4	4.58	3.84×10^{-3}	38.3	5.72	95.9
PEO_{60}: $AgCF_3SO_3$	19.15	4.64	4.88×10^{-3}	30.1	5.8	43.6
PEO_{50}: $AgCF_3SO_3$	19.2	4.62	5.41×10^{-3}	27.2	5.77	98.2

Differential scanning calorimetric (DSC) data

The DSC thermogram traces obtained for $(PEO)_x$:$AgCF_3SO_3$ (where x = 50, 60, 70, 80, 90 and 100 respectively) complexes during heating cycles over the temperature range 200 - 360 K are illustrated in **Fig. 9**. The DSC curve of pure PEO displays a step change at 210 K [-63°C] which may be attributed to the glass transition temperature (T_g) of the polymer host. Upon incorporation of silver triflate (AgTr) salt into the matrix of PEO the value of T_g reaches a maximum value of 221 K [-54°C] for the $(PEO)_{60}$:$AgCF_3SO_3$ complex and this type of increase in glass transition temperature may provide the desirable flexibility of polymer backbone chain in the case of PEO polymer thereby facilitating rapid movement of ionic species which would in turn enhance the electrical conductivity. These features clearly indicate the complexation taking place between PEO polymer and silver triflate salt **[32]**.

From **Fig. 9** it is also obvious that pure PEO exhibits a sharp endothermic melting peak, T_m at 339 K and that after the incorporation of $AgCF_3SO_3$ salt the melting point value gets shifted to 338, 338, 336, 333 and 337 K for $(PEO)_x$:$AgCF_3SO_3$ complexes having x = 50, 60, 70, 80 and 90 respectively. It is also noticed that both the melting point (T_m) and depth of melting dip are gradually reduced for the AgTr-salt doped PEO polymer electrolyte system and this sort of changes occurring in T_m is yet an indication of miscibility and transition of CPE from semi-crystalline to amorphous phase. The relative degree of crystallinity (χ_c) has been calculated as the ratio of enthalpy of fusion of composite polymer electrolyte film experimentally calculated (ΔH_f) to the enthalpy of fusion of pure crystalline PEO phase ($\Delta H°_{PEO}$) hypothetically obtained. The value of $\Delta H°_{PEO}$ is found to be 213.7 Jg^{-1} from the literature point of view [**33**] and the calculated degree of crystallinity ranges between 99.2 % for pure PEO to 44.4 % for $(PEO)_{60}$:$AgCF_3SO_3$ composite polymer electrolyte film. This aspect may be due to the steric hindrance caused by PEO polymer and also Ag^+ cationic species in salt induce restraining effect on the crystallization of PEO and hence decreasing the degree of crystallinity. Interestingly, this kind of decrease in the observed degree of crystallinity represents a remarkable effect on the behavior of electrical conductivity as concurred from the above XRD and conductivity results too.

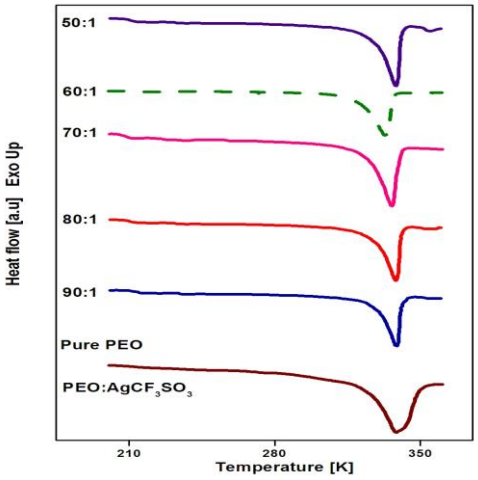

Fig. 9. DSC thermograms of different compositions of $(PEO)_x$:$AgCF_3SO_3$ composite polymer electrolyte complexes.

Morphological and compositional results

Fig. 10 (a) and (b) shows the scanning electron microscopic (SEM) and field emission scanning electron microscopic (FESEM) images of $(PEO)_{60}$:$AgCF_3SO_3$ composite polymer electrolyte sample.

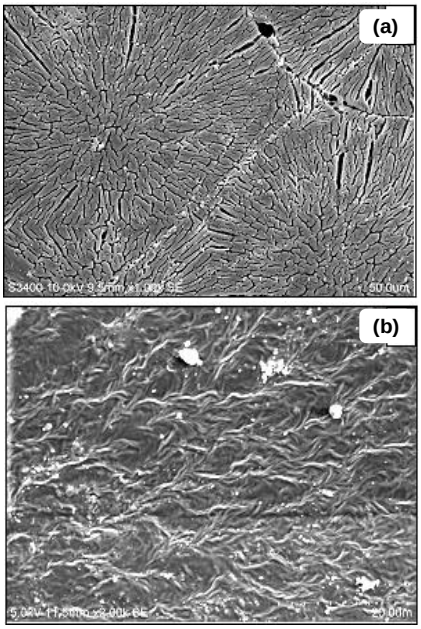

Fig. 10. (a) SEM and (b) FESEM images obtained for the $(PEO)_{60}$:$AgCF_3SO_3$ composite polymer electrolyte film.

Generally, micrographical image of pure PEO shows the presence of several spherulitic crystalline domains closely packed to each other in an orderly manner as reported already [**34**]. However, during the present work, the effect of silver triflate ($AgCF_3SO_3$) salt content on pure PEO polymer has been analyzed. From **Fig. 10 (a)** it is clear that an incredible improvement from crystalline to amorphous phase is found to result after the addition of $AgCF_3SO_3$ salt into the polymer and the existence of small gaps in the boundary between the spherulites is an apparent indication of the existence of an amorphous phase. The FESEM image of pure PEO shows the rough surface morphology with lots of rumples thus indicating the crystalline nature of PEO as reported earlier [**35**] but FESEM image shown in **Fig. 10 (b)** reveals a smooth porous surface with the reduction of rumples due to the incorporation of silver triflate salt and this fact leads to an enhancement in the observed conductivity owing to the reduction in PEO crystallinity.

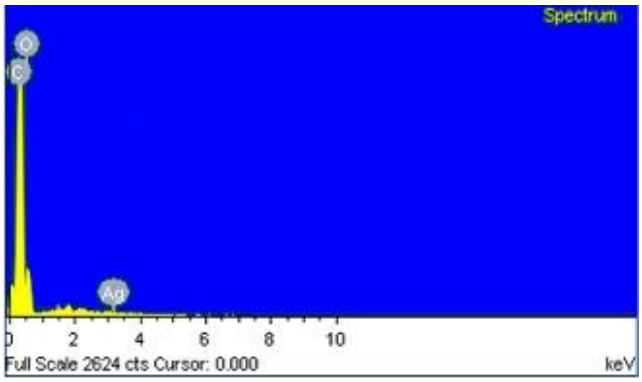

Fig. 11. EDX elemental analysis pattern of $(PEO)_{60}$:$AgCF_3SO_3$ composite polymer electrolyte film.

On the other hand, **Fig. 11** shows the EDX elemental analysis pattern of $(PEO)_{60}$:$AgCF_3SO_3$ composite polymer electrolyte sample, suggesting the necessary and sufficient confirmation of $AgCF_3SO_3$ salt content within the electrolyte film specimen resulting from its complexation with PEO polymer.

Discharge characteristics of a solid state battery

Electrochemical cells with the configuration $Ag/(PEO)_{60}$:$AgCF_3SO_3/I_2$+G+CPE were fabricated and the observed discharge characteristics of the cell at room temperature (298 K) without load and for a constant load of 1 MΩ are shown in **Fig. 12**.

Table 3. Various cell parameters evaluated for the best conducting $(PEO)_{60}$: $AgCF_3SO_3$ composite polymer electrolyte film.

Cell Parameters	Without load	Under a constant load of 1 MΩ
Weight of the cell (g)	0.84	0.75
Area of the cell (cm^2)	0.5024	0.5024
Open circuit voltage (mV)	665	421
Short circuit current (μA)	78.5	93.6
Current density (μA/cm^2)	156.3	186.3
Power density (mW/kg)	62.1	39.4
Time of plateau region (h)	98.5	44.2
Energy density (Wh/kg)	6.12	1.74
Discharge capacity (μA/h)	0.79	2.12

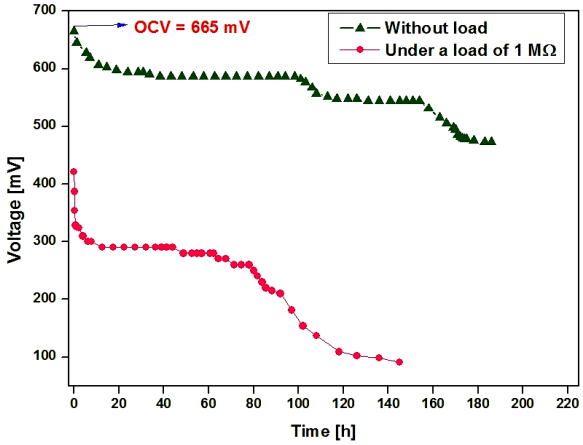

Fig. 12. Discharge curves obtained for the $(PEO)_{60}$: $AgCF_3SO_3$ cell without load and at a constant load of 1 MΩ at room temperature (298 K).

The open-circuit voltage (OCV) and short-circuit current (SCC) of the newly prepared sample without load were found to be 665 mV and 78.5 μA and listed in **Table 3**. These profiles tend to show that the observed decrease in voltage values may be due to the polarization of silver (Ag^+) ions at the electrode-electrolyte interface whereas these parameters demonstrate the potential application of this composite polymer electrolyte for applications in solid-state batteries.

Conclusion

Composite polymer electrolytes (CPEs) based on enriched polyethylene oxide (PEO) polymer content in conjunction with silver triflate ($AgCF_3SO_3$) salt have been developed and investigated. The highest room temperature electrical conductivity of the salted system was found to be 2.9×10^{-5} Scm^{-1} for $(PEO)_{60}$:$AgCF_3SO_3$ CPE film at room temperature (298 K) whereas temperature-dependence of electrical conductivity of the electrolyte obeys Arrhenius relation. The occurrence of reduction in crystallinity has been confirmed from XRD results revealing that the average particle size of the film remaining in nanosize configuration. Furthermore, the DSC analysis has indicated that the addition of salt induces change in melting temperature and decreases the degree of crystallinity which is correlated with XRD features. The fact that the polymer and salt are uniformly dispersed with an increased amorphous nature of the complex as evident from the present SEM, FESEM and EDAX results. An archetype electrochemical cell fabricated using the optimum conducting composition of CPE and its satisfactory performance under low current drains and stable discharge characteristics reveal the chosen complex as a promising candidate for application in solid state batteries.

Acknowledgements

The authors would like to thank National Centre for Nanoscience and Nanotechnology (NCNSNT), University of Madras for SEM analysis and Council of Scientific and Industrial Research, New Delhi for the financial support received in the form of a research project (No. 03(1292)/13/EMR-II Dated 09-4-2013).

Reference

1. Morita, M.; Araki, F.; Yoshimoto, N.; Ishikawa, M.; Tsutsumi, H.; *Solid State Ionics*, **2000,** *136*, 1167.

DOI: 10.1016/S0167-2738(00)00613-5
2. Shahzada, A.; Sharif, A.; Agnihotry, S. A.; *J. Power Sources*, **2005**, *140*, 151. **DOI:** 10.1016/j.jpowsour.2004.08.002
3. Aziz, S. B.; Abidin, Z. H. Z.; Arof, A. K.; *Physica B: Condens. Matt.* **2010**, *405*, 4429. **DOI:** 10.1016/j.physb.2010.08.008
4. Aravindan, V.; Vickraman, P.; *J. Appl. Polym. Sci.*, **2008,** *108*, 1314. **DOI:** 10.1002/app.27824
5. Depifanio, A.; Serraino Flory, F.; Licoccia, S.; Traversa, E.; Scrosati, B.; Croce, F.; *J. Appl. Electrochem.*, **2004,** *34*, 403. **DOI:** 10.1023/B:JACH.0000016623.42147.68
6. Polu, A. R.; Kumar, R.; *Adv. Mat. Lett.*, **2013,** *4*, 543. **DOI:** 10.5185/amlett.2012.9417
7. Ramesh, S.; Liew, C. *Measurement*, **2013,** *46*, 1650. **DOI:** 10.1016/j.measurement.2013.01.003
8. Austin Suthanthiraraj, S.; Kumar, R.; Joseph Paul, B.; *J. Appl. Electrochem.*, **2010,** *40*, 401. **DOI:** 10.1007/s10800-009-0010-4
9. Lee, Y.; Ratner, M. A.; Shriver, D. F.; *Solid State Ionics*, **2001,** *138*, 273. **DOI:** 10.1016/S0167-2738(00)00791-8
10. Choudhary, S.; Sengwa, R. J. *Indian J. Phys.* **2012,** *86*, 335. **DOI:** 10.1007/s12648-012-0063-9
11. Zhang, C.; Qi, D. J.; Zhang, X. C.; Fang, Q. K.; Wu. S. J.; Sun, B. H.; *Adv. Mater. Res.* , **2014,** *850-851*, 28-31. **DOI:** 10.4028/www.scientific.net/AMR.850-851.28
12. Lee, L.; Kim, I.; Yang, S.; Kim, S.; *Res. Chem. Intermed.*, **2013,** *39*, 3279. **DOI:** 10.1007/s11164-012-0839-8
13. Carrilho Plancha, M. J.; Rangel, C. M.; Correia de Sequeira, C. A.; *J. Solid State Electrochem.*, **2012,** *16*, 665. **DOI:** 10.1007/s10008-011-1406-8
14. Serra Moreno, J.; Armand, M.; Berman, M. B.; Greenbaum, S. G.; Scrosati, B.; Panero, S.; *J. Power sources*, **2014,** *248*, 695. **DOI:** 10.1016/j.jpowsour.2013.09.137
15. Reddeppa, N.; Sharma, A. K.; Narasimha Rao, V. V. R.; Chen, W.; *Measurement*, **2014,** *47*, 33. **DOI:** 10.1016/j.measurement.2013.08.047
16. Rajendran, S.; Kannan, R.; Mahendran, O.; *J. Power Sources*, **2001,** *96*, 406. **DOI:** 10.1016/S0378-7753(00)00573-5
17. Kunteppa, H.; Roy, A. S.; Devendrappa, H.; Ambika Prasad, M. V. N.; *J. Appl. Polym. Sci.*, **2012,** *125*, 1652. **DOI:** 10.1002/app.34825
18. Sarada, B. A.; Balaji Bhargav, P.; Sharma, A. K.; Rao, V. V. R. N.; *Mater. Res. Innov.*, **2011,** *15*, 394. **DOI:** 10.1179/143307511X13189528030753
19. Klongkan, S.; Pumchusak, J.; *Electrochim. Acta*, **2015**, *161*, 171. **DOI:** 10.1016/j.electacta.2015.02.074
20. Nimah, Y. L.; Cheng, M.; Cheng, J. H.; Rick, J.; Hwang, B. *J.; Power Sources*, **2015**, *278*, 375. **DOI:** 10.1016/j.jpowsour.2014.11.047
21. Sengwa, R. J.; Dhatarwal, P.; Choudhary, S.; *Curr. Appl. Phys.*, **2015**, *15*, 135. **DOI:** 10.1016/j.cap.2014.12.003
22. Kwon, S.; Kim, D.; Shim, J.; Lee, J. H.; Baik, J.; Lee, J.; *Polymer* , **2014**, *55*, 2799. **DOI:** 10.1016/j.polymer.2014.04.051
23. Aziz, S. B.; Abidin, Z. H. Z.; Arof, A. K.; *Physica B: Condens. Matt.*, **2010**, *405*, 4429. **DOI:** 10.1016/j.physb.2010.08.008
24. Gondaliya, N.; Kanchan, D. K.; Sharma, P.; Jayswal, M. S.; *Polym. Compos.*, **2012**, *33*, 2195. **DOI:** 10.1002/pc.22362
25. Polu, A. R.; Kim, D. K.; Rhee, H. *Ionics* 2015, In press. **DOI:** 10.1007/s11581-015-1474
26. Aziz, S. B.; Abidin, Z. H. Z.; Arof, A. K.; *EXPRESS Polym. Lett.*, **2010,** *4*, 300. **DOI:** 10.3144/expresspolymlett.2010.38
27. Ibrahim, S.; Yasin, S. M. M.; Nee, N. M.; Ahmad, R.; Johan, M. R.; *Solid State Commun.*, **2012,** *152*, 426. **DOI:** 10.1016/j.ssc.2011.11.037
28. Rajarajan, K.; Selvakumar, S.; Joseph, G.P.; Vedha Potheher, I.; Gulam Mohamed, M.; Sagayaraj, P.; *J. Cryst. Growth*, **2006,** *286*, 470. **DOI:** 10.1016/j.jcrysgro.2005.10.092
29. Jaipal Reddy, M.; Chu, P. P.; *Solid State Ionics*, **2002,** *149*, 115. **DOI:** 10.1016/S0167-2738(02)00141-8
30. Mohapatra, S. R.; Thakur, A. K.; Choudhary, R. N. P.; *Ionics*, **2008,** *14*, 255. **DOI:** 10.1007/s11581-007-0171-2
31. Abdel kader, F. H.; Hakeem, N. A.; Elashmawi, I. S.; Ismail, A. M.; *Indian J. Phys.*, **2013,** *87*, 983. **DOI:** 10.1007/s12648-013-0333-1
32. Zhao, Y.; Tao, R.; Fujinami, T.; *Electrochim. Acta*, **2006,** *51*, 6451. **DOI:** 10.1016/j.electacta.2006.04.030
33. Tang, Z.; Wang, J.; Chen, Q.; He, W.; Shen, C.; Mao, X.; Zhang, J.; *Electrochim. Acta*, **2007,** *52*, 6638. **DOI:** 10.1016/j.electacta.2007.04.062
34. Hu, L.; Tang, Z.; Zhang, Z. *J.; Power Sources*, **2007,** *166*, 226. **DOI:** 10.1016/j.jpowsour.2007.01.028
35. Noor, S. A. M.; Ahmad, A.; Talib, I. A.; Rahman, M. Y. A.; *Ionics*, **2010,** *16*, 161. **DOI:** 10.1007/s11581-009-0385-6